Ilam University of Medical Sciences

Plant Biotechnology Persa

Online ISSN: 2676-7414

Homepage: https://pbp.medilam.ac.ir

Evaluating Antagonistic Inhibitory Effect of Some Antibiotic–Silver Nanoparticle Combinations

Mustapha Isah[1,2]✉, **Shafiu Abdullahi Namadi**[2], **Fatimah Ibrahim Jumare**[1,3]

[1]Department of Biosciences, Faculty of Science, Universiti Teknologi Malaysia, 81310 UTM Skudai, Johor, Malaysia
[2]Department of Biochemistry and Molecular Biology, Sokoto State University, Birnin Kebbi Rd, Sokoto PMB 2134, Sokoto, Nigeria
[3]Department of Microbiology, Sokoto State University, Birnin Kebbi Rd, Sokoto PMB 2134, Sokoto, Nigeria

Article Info

Article type:
Original Article

Article History:
Received: 25 Aug 2025
Revised: 04 Sep 2025
Accepted: 02 Sep 2025
Published Online:

✉ ***Correspondence to:***
Mustafa Isah

Email:
imustapha@graduate.utm.my

A B S T R A C T

Objective: This study reports on the green synthesis of silver nanoparticles (AgNPs) using *Moringa oleifera* leaf extract as a natural reducing and stabilizing agent. The AgNPs were combined with some antibiotics to determine the antibacterial mode of inhibition.

Methods: The synthesized AgNPs were comprehensively characterized by UV–visible spectroscopy, X-ray diffraction (XRD), Fourier transform infrared spectroscopy (FTIR), field emission scanning electron microscopy (FESEM), energy dispersive X-ray spectroscopy (EDX), transmission electron microscopy (TEM), and zeta potential (ZP) analysis followed by combination with some selected antibiotics by soaking the designated antibiotic discs in to the AgNPs colloidal and assessed their mode of inhibition.

Results: The characterization confirmed the formation of uniformly distributed, spherical AgNPs with size ranging from 15 to 30 nm, and a negative surface charge of –27.1 mV, indicating a high colloidal stability. To investigate their biomedical relevance, AgNPs were combined with conventional antibiotics through soaking of the antibiotic discs into colloidal AgNPs, and tested against *Staphylococcus aureus (S. aureus*), methicillin-resistant *S. aureus* (MRSA), *Escherichia coli* (*E. coli*), and *Pseudomonas aeruginosa* (*P. aeruginosa*) using the Disc diffusion test (DDT). The result of combining AgNPs with an antibiotic showed a reduction in inhibition zones compared to the zones observed when the antibiotic was used alone against all bacterial strains tested.

Conclusion: The results of AgNPs–antibiotic combinations showed decreased in inhibition zones which is refers to antagonistic behaviour instead of increase in the zones diameter indicating a synergistic behaviour as often reported. These results highlight the potential of *M. oleifera*-mediated AgNPs as an environmentally friendly nanomaterial to enhance antibiotic activity but also emphasize the need for critical evaluation of nanoparticle–drug interactions prior to clinical application.

Keywords: *Moringa oleifera*, Silver nanoparticles, Green synthesis, Multi-resistant drugs, Antibacterial effect

➢ **How to cite this paper**
Isah M, Namadi SA, Jumare FI. Evaluating antagonistic inhibitory effect of some antibiotic–silver nanoparticle combinations. Plant Biotechnology Persa. 2026; 8(1): DOI: 10.61882/pbp.8.1.12

[DOI: 10.61882/pbp.8.1.12]

Introduction

The swift rise of multidrug-resistant (MDR) pathogens has become a critical global health threat [1]. This situation could undermine the effectiveness of conventional antibiotics and complicating infection management. The indiscriminate use of antibiotics in clinical settings has accelerated the development of resistance instruments such as efflux pumps [2], enzymatic degradation, and biofilm development [3]. As a result, once treatable infections are becoming increasingly difficult to control, leading to prolonged hospitalization, higher treatment costs, and significant mortality rates [4]. Addressing this crisis requires the development of innovative antibacterial strategies that can restore or improve the efficacy of existing antibiotics.

The synthesis of AgNPs using plant-derived materials offers a sustainable, eco-friendly approach. The phytochemicals in *M. oleifera* leaves (flavonoids, phenols, alkaloids, and proteins) act as natural reducing and stabilizing agents, eliminating the need for toxic chemicals [5]. Nano-based antimicrobials, particularly AgNPs, have gained attention as promising candidates due to

DOI: 10.61882/pbp.8.1.12
Publisher: Ilam University of Medical Sciences

their broad-spectrum antibacterial activity and unique physicochemical properties. AgNPs can interact with microbial cells through multiple pathways, including disruption of membranes, generation of reactive oxygen species (ROS) [6], and release of silver ions (Ag^+), that interfere with proteins and nucleic acids [7]. These combined effects eventually lead to denaturation of proteins, inhibition of essential enzymatic processes, impairment of DNA replication and transcription and finally to cell death. In contrast to single-target antibiotics, this multi-coated mechanism reduces the likelihood of rapid resistance development. However, AgNPs alone are not without limitations, including dose-dependent cytotoxicity and potential instability in biological environments, emphasizing the need for hybrid approaches that balance efficacy and safety.

One strategy that has attracted considerable interest is the combination of AgNPs with conventional antibiotics to exploit potential synergistic effects [8]. Theoretically, such combinations can enhance antibacterial activity through complementary mechanisms, thus lowering the required dosage of each drug, reducing toxicity, and overcoming resistance barriers. However, recent studies show that these interactions are not always synergistic. Some combinations lead to neutral or even antagonistic effects, where antibacterial activity is reduced compared to the agents used alone. This two-fold nature highlights a complex interplay between the surface chemistry of the nanoparticles, the antibiotic class, and the microbial physiology, that is not yet fully understood.

This study systematically evaluates the antibacterial effects of selected antibiotic-AgNP combinations, highlighting the antagonistic behaviour of interaction when some antibiotics are combined with AgNPs instead of showing synergistic effect as previous studies reported. Understanding whether such interactions lead to synergistic enhancement or antagonistic interference is crucial for rational application in biomedical contexts. The present study therefore investigates the antibacterial inhibitory effects of selected antibiotic–AgNPs combinations and provides experimental evidence for antagonistic outcomes. By elucidating these opposing interactions, the work closes an important knowledge gap and contributes to the informed development of hybrid therapeutics of nanoparticles and antibiotics to combat antimicrobial resistance.

Material and Methods

Materials and Chemicals

Moringa oleifera leaves powder from Nanomaterial laboratory 1, T02, UTM, microbial strains from American Type Culture Collection (ATCC), antibiotic discs (Thermo Scientific), silver nitrate ($AgNO_3$) (VWR), Mueller Hinton agar (MHA) (Sigma Life Science), sodium hydroxide (NaOH) QReC (Asia), distilled water filtrate of sartorius filter (Malaysia Sdn Bhd, 98806).

Extraction of plant resource

A measured quantity of 5 g of *M. oleifera* leaf powder was added to 50 mL of distilled water and heated with a magnetic stirrer while stirring continuously until the mixture reached the boiling point. The solution was kept at the boiling point for 15 minutes to facilitate the extraction of the phytoconstituents. The mixture was allowed to cool to room temperature prior to filtration through Whatman No. 1 filter paper. The filtrate was adjusted to a pH of 8 to enhance the ionization of the reducing species for subsequent applications.

Preparation of silver precursor

A stock solution of silver nitrate ($AgNO_3$) was prepared by dissolving 0.85 gram of $AgNO_3$ in 500 mL of distilled water with constant stirring to ensure complete solubilization. The solution was then covered with aluminium foil to prevent photodegradation of silver ions and subsequently stored under suitable conditions for prior use.

Preparation of AgNPs

A volume of 5 mL of *M. oleifera* leaf extract was added to 500 mL of $AgNO_3$ solution and the mixture was incubated in the dark for 24 hours to facilitate the reduction of Ag^+. The formation of AgNPs was indicated by the presence of a dark brown colour, after which the colloid was subjected to characterization. For the antimicrobial test, each antibiotic disc was immersed in 1 mL of the AgNPs colloid suspension followed by oven dried at 50 °C for 15 minutes. The AgNP-impregnated discs were then used for the subsequent antibacterial analysis.

Characterization techniques

The synthesized AgNPs was characterized using techniques such as UV– visible spectrophotometry, FTIR, XRD, FESEM, EDX, TEM, and ZP measurements as seen in Table 1. All the analyses were conducted at University Laboratory Management Centre, T03, UTM except for UV-visible which was performed at Nanomaterial Laboratory 1, T02, UTM using Janway 7200 spectrophotometer. FTIR spectra were recorded using a Nicolet IS5 IR spectrometer (Thermo Scientific, USA) and OMNIC software. Sample preparation was performed using the KBr pellet method to ensure reliable and reproducible infrared absorption data. X-ray diffraction patterns were recorded using a Bruker D8 Advance diffractometer with Cu Kα radiation (λ = 1.5406 Å). The device was operated at 40 kV and 20 mA, with data acquired over a 2θ angle range of 5°-90°. Scans were performed with a step size of 0.05°, a scan speed of 0.05° per second and using 0.5° divergence [9], and anti-scattering slits to improve resolution and reduce background noise.

The elemental composition was determined using EDX in conjunction to enable spatially resolved elemental mapping of the sample surfaces. The EDX data was collected in a multi-step procedure that included large-area imaging of the sample, targeted spot analyses and both qualitative and quantitative elemental assessments. All EDX measurements were performed using a Hitachi SU8020 field emission scanning electron microscope equipped with an integrated EDX detector to ensure high-resolution elemental mapping and compositional analysis. TEM was performed with a Hitachi HT7700 device operating at an accelerating voltage of 120 kV. This microscope offers nanoscale imaging capabilities with a grating resolution of 0.204 nm (at 100 kV) and supports magnifications up to 200,000×. Imaging was performed with an 8-megapixel camera system,

[DOI: 10.61882/pbp.8.1.12]

which enables detailed structural characterization of the morphology and distribution of the nanoparticles. The ZP was measured with the Malvern Zetasizer using electrophoretic light scattering and laser Doppler velocimetry [10]. The device applies an electric field to a sample, causing charged particles to move. Based on the speed of this movement, and the properties of the sample, such as viscosity and dielectric constant, the Zetasizer can calculate the zeta potential. The characterization techniques used are summarized below:

Table 1. Characterization techniques used for synthesized AgNPs

Technique	Instrument/Model	Operating Conditions/Details	Purpose/Information Obtained	Location
UV–Visible	Janway 7200 spectrophotometer	Conducted at room temperature	Surface plasmon resonance (SPR) analysis to confirm AgNP formation and optical properties	Nanomaterial Laboratory 1, T02, UTM
FTIR	Nicolet IS5 IR spectrometer (Thermo Scientific, USA) with OMNIC software	KBr pellet method; spectra recorded in mid-IR region	Identification of functional groups involved in capping, stabilization, and reduction of AgNPs	University Laboratory Management Centre, T03, UTM
XRD	Bruker D8 Advance diffractometer with Cu Kα radiation (λ = 1.5406 Å)	40 kV, 20 mA; 2θ = 5°–90°; step size = 0.05°; scan speed = 0.05°/s; 0.5° divergence and anti-scattering slits	Determination of crystalline structure, phase purity, crystallite size	University Laboratory Management Centre, T03, UTM
FESEM-EDX	Hitachi SU8020 FESEM with integrated EDX detector	EDX analysis included large-area imaging, spot analysis, and qualitative/quantitative elemental mapping	Morphological analysis and elemental composition of AgNPs	University Laboratory Management Centre, T03, UTM
TEM	Hitachi HT7700 TEM	Accelerating voltage: 120 kV; resolution: 0.204 nm (at 100 kV); magnification: up to 200,000×; 8 MP camera system	High-resolution imaging of nanoparticle morphology, size distribution, and structural features	University Laboratory Management Centre, T03, UTM
ZP	Malvern Zetasizer	Electrophoretic light scattering and laser Doppler velocimetry	Surface charge, colloidal stability, and dispersion behavior of AgNPs	University Laboratory Management Centre, T03, UTM

Antibacterial Test

Disc Diffusion Test

The antibacterial activities of AgNPs, Chloramphenicol (CHL) and cefoxitin (FOX) singly and in combination with AgNPs were evaluated using disc diffusion technique (DDT) against American Type Cell Culture (ATCC) *S. aureus* (6538), *E. coli* (11229), *Pseudomonas aeruginosa* (65442), and MRSA (43300). Bacterial cultures were grown on Mueller–Hinton agar (MHA), and standardized inoculum were prepared by suspending isolated colonies in sterile saline and adjusting

[DOI: 10.61882/pbp.8.1.12]

turbidity to 0.5 McFarland standard, which corresponds to ~1.5 × 10^8 CFU/mL. The suspensions were spread evenly onto fresh MHA plates using sterile cotton swabs to ensure uniform inoculation for proper antimicrobial testing. CLSI M100: Performance Standards for Antimicrobial Susceptibility Testing was used as reference guidelines.

The inoculated plates with the test samples were incubated at 37 °C for 18–24 hours. After incubation, the antibacterial activity was evaluated by measuring the diameter of the inhibition zone around each disc in millimeters (mm) using a ruler performed in triplicates. The resultant was reported as mean and standard deviation of the mean. This measurement served as an indicator of the effectiveness of the test samples in inhibiting bacterial growth.

Results

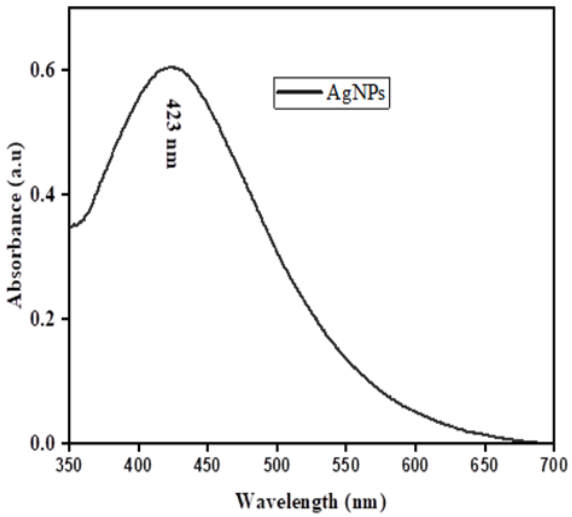

Figure 1. Shows the UV–Vis spectrum of AgNPs, demonstrating a SPR peak at 423 nm indicative of nanoparticle formation

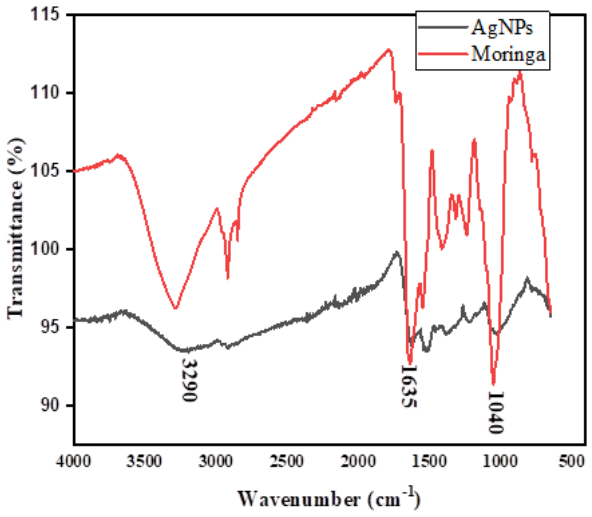

Figure 2. (a) FT-IR analysis showing the reduced bands upon comparing Moringa leaves powder (red), and (b) AgNPs (black)

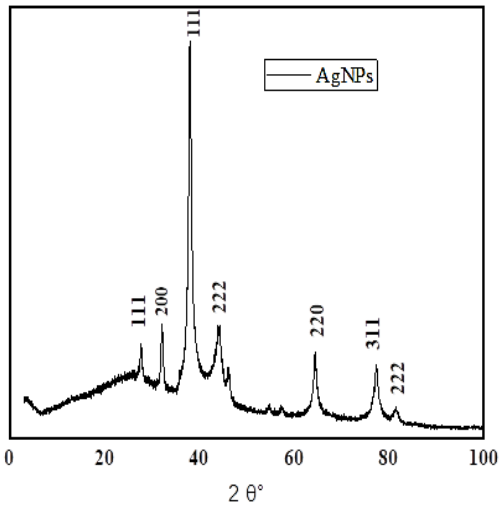

Figure 3. XRD analysis of AgNPs shows the crystallinity nature of the synthesized AgNPs

[DOI: 10.61882/pbp.8.1.12]

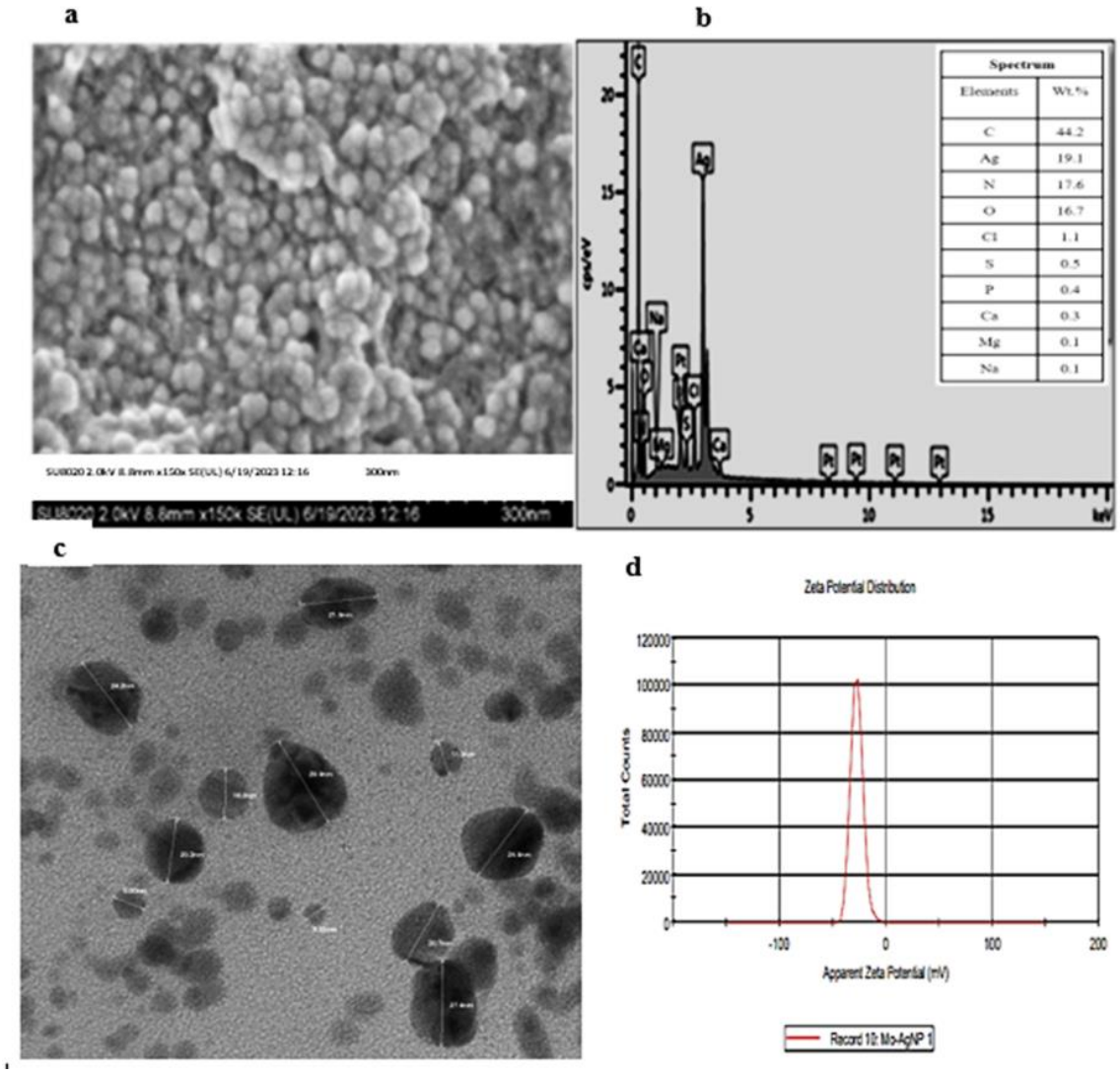

Figure 4. (a) FESEM image shows the shape, (b) EDX spectra shows the elemental composition, (c) HRTEM shows the size range and (d) Zeta potential shows the dispersity of AgNPs

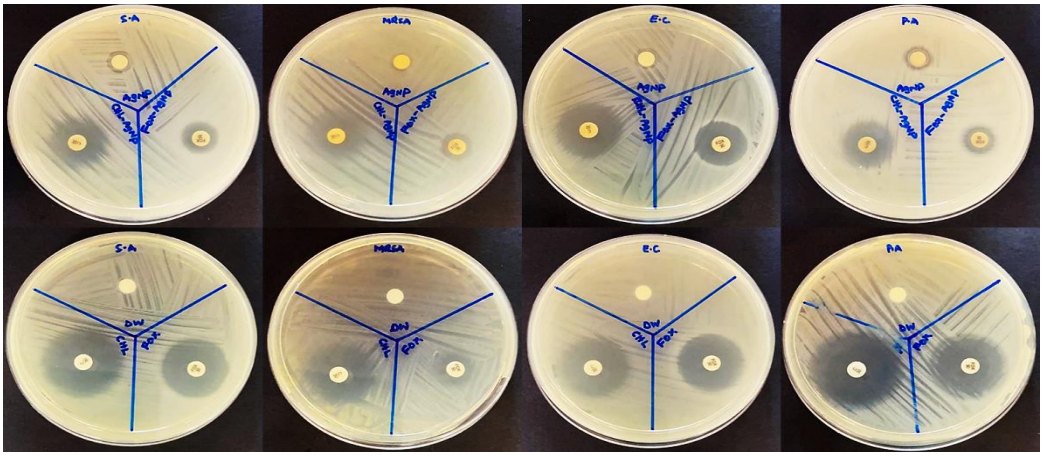

[DOI: 10.61882/pbp.8.1.12]

Figure 2. Test samples showing the inhibition zones AgNPs alone, antibiotic alone, and in their combination state.

Table 2. Disc diffusion result of antibiotic-silver nanoparticles

Antibiotics/AgNP	Zone of inhibition (mm)			
	S. aureus	MRSA	*E. coli*	*P. aeruginosa*
FOX only	23 ±1.0	12 ± 0.0	23 ± 1.0	25 ± 0.0
CHL only	28 ± 1.0	25 ± 0.0	27 ± 1.0	31 ± 1.0
AgNP only	9 ± 0.0	8 ± 0.5	9 ± 0.0	10 ± 0.0
FOX-AgNP	12 ± 0.0	11 ± 0.0	17 ± 0.0	12 ± 0.0
CHL-AgNP	18 ± 0.0	13 ± 0.0	24 ± 1.0	20 ± 1.0

FOX = Cefoxitin, CHL = Chloramphenicol, AgNP = Silver nanoparticle results; n =3, values are Mean ± SD

Discussion

AgNP formation was proven by adding 5 mL of *M. oleifera* leaf extract to 500 mL of 1.0 mM $AgNO_3$ solution, which produced a gradual colour shift from pale yellow to dark brown. This visual change serves as an initial confirmation of nanoparticle synthesis, attributed to surface plasmon resonance (SPR) generated by the collective oscillation of conduction electrons on the nanoparticle surface under light exposure [11].

UV–Visible spectrophotometric analysis also confirmed the successful reduction of Ag^+ ions to AgNPs. As shown in Figure 1, the absorption spectrum of the colloidal suspension revealed a characteristic SPR peak at 423 nm, which is within the well-established range (400–480 nm) typically reported for spherical silver nanoparticles [12]. The sharpness and symmetry of the peak indicate the formation of nanoparticles with relatively uniform size distribution, while the absence of additional peaks rules out the presence of significant impurities or secondary products.

The absorption intensity observed in the spectrum also reflects the concentration of nanoparticles formed in the reaction medium. Higher absorbance at the SPR peak indicates efficient nucleation and growth of AgNPs, which is favoured by the phytochemicals present in *M. oleifera* leaves extract acting as both reducing and stabilizing agents. Polyphenols, flavonoids, and other biomolecules present in the extract are known to donate electrons for Ag^+ reduction while capping the nanoparticles, which prevents uncontrolled agglomeration [13]. Overall, the visible colour change coupled with the distinct SPR peak at 423 nm is strong evidence for the successful green synthesis of AgNPs with *M. oleifera* extract. These results confirm the dual role of the plant extract as a natural bioreductant and stabilizer and underline its potential as an eco-friendly and cost-effective approach for the synthesis of nanomaterials. Further characterisations, such as DLS or ZP, FTIR, and TEM, would be necessary to elucidate particle size distribution, surface chemistry, and morphology to complement the spectrophotometric evidence.

The table below shows the interpreted results of physicochemical parameters of the synthesized AgNPs which was confirmed by several physicochemical characterisation techniques as shown in Table 3.

Table 3. Interpretation of physicochemical results of AgNPs synthesized using *M. oleifera* extract.

Characterization Technique	Key Findings	Interpretation
FTIR Spectroscopy	Absorption bands at ~3290 cm^{-1} (O–H), 1635 cm^{-1} (C=O), and 1040 cm^{-1} (C–O), with shifts and intensity changes after nanoparticle formation.	Confirms the involvement of phenolic, flavonoid, and protein groups in reduction and capping. Phytochemicals act as bioreductants and stabilizers, preventing agglomeration.
X-ray Diffraction (XRD)	Distinct peaks at 2θ ≈ 38°, 44°, 64°, 77°, corresponding to (111), (200), (220), and (311) planes of FCC silver (JCPDS No. 04-0783).	Sharp peaks indicate crystalline nature of AgNPs; minor additional peaks suggest residual plant-derived stabilizing compounds.
FESEM & EDX	FESEM: Nanoparticles aggregated but relatively uniformly distributed at nanoscale. EDX: Strong Ag signal (19.1 wt%) with C, O, N, and trace Cl, S, P, Mg.	FESEM reveals morphology and distribution; EDX confirms elemental composition and phytochemical-based capping.
TEM	Predominantly spherical nanoparticles with size range ~15–30 nm; clear lattice fringes visible.	Confirms nanoscale dimensions, crystalline nature, and effective phytochemical stabilization consistent with UV–Vis and XRD results.

[DOI: 10.61882/pbp.8.1.12]

Zeta Potential (ZP)	Average surface potential: –27.1 mV.	Indicates good colloidal stability due to electrostatic repulsion and steric hindrance from plant stabilizers; suitable for biological applications.

The antibacterial efficacy of cefoxitin (FOX), chloramphenicol (CHL), silver nanoparticles (AgNPs), and their respective combinations was assessed using the DDT against four representative bacterial strains: *S. aureus*, MRSA, *E. coli*, and *P. aeruginosa* as shown in figure 1 and Table 3 respectively.

As expected, both antibiotics alone showed strong antibacterial activity, with inhibition zones of 12–31 mm. CHL showed the greatest efficacy in all strains, with inhibition diameter of 28 mm (*S. aureus*) and 31 mm (*P. aeruginosa*), consistent with its broad spectrum of activity [8]. In contrast, AgNPs alone showed relatively weak inhibition (8–10 mm), suggesting a moderate stand-alone antimicrobial effect, which is consistent with previous reports of lower efficacy of AgNPs in independent testing [14].

The antibacterial assay in Table 2 showed that both FOX and CHL exhibited significant inhibitory activity, with CHL consistently producing larger zones of inhibition than FOX, particularly against *P. aeruginosa* (31 mm) and MRSA (25 mm). In contrast, AgNPs alone showed only weak antibacterial effects (8–10 mm) against all strains, indicating their limited efficacy as a stand-alone antimicrobial agent. Interestingly, the overall inhibitory activity decreased rather than improved when AgNPs, were combined with the antibiotics. Inhibition zones were significantly reduced with FOX-AgNPs compared to FOX alone for all bacteria tested (e.g., 12 mm vs. 23 mm for *S. aureus*; 11 mm vs. 12 mm for MRSA), clearly indicating an antagonistic interaction in which the presence of AgNPs reduces FOX activity. Similarly, CHL–AgNPs combinations showed reduced zones of inhibition compared to CHL alone, with decreased levels against *E. coli* (24 mm vs. 27 mm) and *P. aeruginosa* (20 mm vs. 31 mm). Although moderate inhibition was still observed against *S. aureus* (18 mm vs. 28 mm) and MRSA (13 mm vs. 25 mm), the reduction compared to CHL alone suggests partial antagonism rather than synergism. Overall, these results emphasize that, the tested AgNP-antibiotic combinations have antagonistic effects contrary to the often-expected synergistic enhancement, which underlines the need for a critical evaluation of nanoparticle–drug interactions prior to therapeutic applications. Although the increase was not dramatic, the enhanced inhibition zones suggest that AgNPs improve drug uptake or facilitate membrane disruption, thereby modestly increasing the efficacy of chloramphenicol [15]. The literature in table 4 indicated the results obtained upon combination of antibiotics with AgNPs.

Table 4. Some Related Literatures on Antibiotic-AgNPs effect against certain bacterial strains

Bacterium/Context	Antibiotic(s) tested with AgNPs	Reported interaction	Notes (assay/metrics)	Reference
Pseudomonas aeruginosa (ATCC + 11 CF isolates)	Imipenem, ceftazidime, ciprofloxacin, levofloxacin, rifampicin	Mostly synergistic; some indifferent (e.g., ceftazidime in a subset)	Disc diffusion + MIC; combinations enlarged zones and lowered MICs; a few isolates showed no interaction with ceftazidime.	[16]
Mixed Gram-negatives (carbapenem-resistant: *E. coli, Klebsiella* spp., *P. aeruginosa, A. baumannii, Proteus* sp.)	β-lactams (ceftriaxone, cefepime, ceftazidime, imipenem)	Synergistic (FIC ≤ 0.5) or partial synergy across panels; no antagonism observed	Checkerboard FICI; cefepime + AgNPs showed the strongest synergy in several isolates.	[17]
Multiple species (focus on aminoglycoside potentiation)	Amikacin, gentamicin (± other aminoglycosides)	Synergistic (marked MIC reduction; ~22-fold in some tests)	MIC, growth kinetics; non-toxic AgNP levels potentiated aminoglycosides substantially.	[18]
Pseudomonas aeruginosa (lab strain MPAO1)	Meropenem, gentamicin, ciprofloxacin with AgNPs/$AgNO_3$ (as "silver" comparators)	Antagonistic with meropenem + AgNP/$AgNO_3$; synergistic with gentamicin	Bliss interaction scores from growth-rate assays; silver–meropenem antagonism was strain- and biocide-specific.	[19]

Although the present disc diffusion assay provides preliminary evidence that the combination of antibiotics with AgNPs resulted in reduced zones of inhibition compared to antibiotics alone, it is important to emphasize that the CLSI and EUCAST guidelines do not provide interpretable breakpoints for AgNPs or for antibiotic–AgNPs combinations. Standardized breakpoints are only available for approved antimicrobial agents, and therefore the inhibition zones observed for AgNPs cannot be classified as susceptible, intermediate, or resistant. Furthermore, disc diffusion is not a validated method to assess antimicrobial interactions such as synergy or antagonism. According to internationally recognized standards, the assessment of interactions between drugs or between drugs and nanoparticles requires quantitative methods, such as

[DOI: 10.61882/pbp.8.1.12]

checkerboard microdilution tests, in which the interaction is expressed as a fractional inhibitory concentration index (FICI). Conventionally, FICI values of ≤0.5 indicate synergy, >0.5–4.0 indicate indifference, and >4.0 indicate antagonism (CLSI M07; EUCAST, 2024). In addition, time–kill assays are recommended to confirm these interactions by assessing the kinetics of bacterial viability over time. Nanoparticles, due to their high surface area and unique physicochemical properties, have recently attracted considerable attention in various fields, including pharmaceuticals, medicine, and microbiology, as effective agents for enhancing drug performance and bioactivity[20-26].

Conclusion

Green synthesis of AgNPs using *M. oleifera* extract was successfully achieved, with phytochemicals mediating both reduction and stabilization, as confirmed by optical, structural, morphological, and stability analyses. The nanoparticles were crystalline, spherical (15–30 nm), and moderately stable, highlighting their potential for biomedical applications. However, when combined with FOX or CHL, AgNPs produced reduced inhibition zones compared to antibiotics alone, indicating predominantly antagonistic interactions, with only an indifferent effect observed for CHL–AgNPs against *E. coli*. These findings suggest that nanoparticle–antibiotic hybrids are not inherently synergistic, as their efficacy depends on nanoparticle surface chemistry, antibiotic mode of action, and microbial physiology. Given the study's limitation to *in vitro* disc diffusion and a narrow antibiotic panel, further research using checkerboard, time–kill, and in vivo models is essential to accurately determine whether AgNPs enhance, diminish, or have no effect on antibiotic activity before advancing clinical applications.

Conflict of interest

The authors declare that they have no known competing financial interests or personal relationships that could have appeared to influence the work reported in this paper.

Ethics declaration

Not applicable

Funding declaration statement

No fund incurred

Acknowledgments

The authors wish to express their gratitude to the TET-FUND Nigeria for fellowship during which the data was obtained.

Declaration of Generative AI and AI assistant tools

As we are not native speakers, we have used ChatGPT 4.0 and Instatext for grammar checking and paraphrasing. The content has been reviewed and edited where necessary, and we take full responsibility for it.

Reference

1. Alara JA, Alara OR. An overview of the global alarming increase of multiple drug resistant: a major challenge in clinical diagnosis. Infect Disord Drug Targets. 2024;24(3):26–42. doi:10.2174/1871526523666230725103902
2. Sinha S, Upadhyay LSB. Understanding antimicrobial resistance (AMR) mechanisms and advancements in AMR diagnostics. Diagn Microbiol Infect Dis. 2025;116949. doi:10.1016/j.diagmicrobio.2025.116949
3. Sonkar V, Devtalla H, Kumar S. Pesticide-driven antimicrobial resistance in water bodies: insights on environmental concerns, health implications and mitigation strategies. Environ Geochem Health. 2025;47(7):282. doi:10.1007/s10653-025-02600-y
4. Ehsan H, Wardak FR, Karimi H, Kamal F, Aminpoor H, Salam A, et al. Comprehensive narrative analysis of antimicrobial resistance in Afghanistan: key drivers, challenges, and strategic interventions. J Health Popul Nutr. 2025;44(1):265. doi:10.1186/s41043-025-00909-z
5. Isah M, Malek NAN, Susanto H, Asraf MH, Matmin J. Determination of essential factors affecting silver nanoparticle synthesis using Moringa oleifera leaves. BIO Web Conf. 2024;117:01005. doi:10.1051/bioconf/202411701005
6. Do HTT, Nguyen NPU, Saeed SI, Dang NT, Doan L, Nguyen TTH. Advances in silver nanoparticles: unraveling biological activities, mechanisms of action, and toxicity. Appl Nanoscience. 2025;15(1):1. doi:10.1007/s13204-024-03076-5
7. Nemčeková K, Dudoňová P, Holka T, Balážová S, Hornychová M, Szebellaiová V, et al. Silver nanoparticles for biosensing and drug delivery: a mechanical study on DNA interaction. Biosensors. 2025;15(5):331.
8. Hadi AA, Malek NAN, Matmin J, Asraf MH, Susanto H, Din SM, Shamsuddin M. Synergistic antibacterial effect of Persicaria odorata synthesised silver nanoparticles with antibiotics on drug-resistant bacteria. Inorg Chem Commun. 2024;159:111725. doi:10.1016/j.inoche.2023.111725
9. Thamilselvan V, Balu S, Ganapathy D, Atchudan R, Arya S, Hazra S, Sundramoorthy AK. Utilization of biomass waste derived carbon quantum dots intercalated ZnO for effective photocatalytic degradation of methylene blue. Results Surf Interfaces. 2025;19:100520. doi:10.1016/j.rsurfi.2025.100520
10. Garg S, Patel P, Gupta GD, Kurmi BD. Pharmaceutical applications and advances with zetasizer: an essential analytical tool for size and zeta potential analysis. Micro Nanosyst. 2024;16(3):139–154. doi:10.2174/0118764029301470240603051432

[DOI: 10.61882/pbp.8.1.12]

11. Yoon H, Kim S, Kim HY. Modulating localized surface plasmon resonance through metal composition and nanoparticle shape: Implications for solar cell applications. Mater Sci Semicond Process. 2025;197:109677. doi:10.1016/j.mssp.2025.109677
12. Shamsoddini SM, Davoudi M, Shahbazi S, Karizi SZ. Green synthesis of silver nanoparticles using Acroptilon repens aqueous extract and their antibacterial efficacy against multidrug-resistant Acinetobacter baumannii. Mol Biol Rep. 2025;52(1):47. doi:10.1007/s11033-024-10156-w
13. Shahzadi S, Fatima S, Shafiq Z, Janjua MRSA. A review on green synthesis of silver nanoparticles (SNPs) using plant extracts: a multifaceted approach in photocatalysis, environmental remediation, and biomedicine. RSC Adv. 2025;15(5):3858–3903. doi:10.1039/D4RA07519F
14. Ifijen IH, Awoyemi RF, Faderin E, Akobundu UU, Ajayi AS, Chukwu JU, et al. Protein-based nanoparticles for antimicrobial and cancer therapy: implications for public health. RSC Adv. 2025;15(19):14966–15016. doi:10.1039/D5RA01427A
15. Singh R, Shedbalkar UU, Wadhwani SA, Chopade BA. Bacteriagenic silver nanoparticles: synthesis, mechanism, and applications. Appl Microbiol Biotechnol. 2015;99(11):4579–4593. doi:10.1007/s00253-015-6622-1
16. Al-Momani H, Albalawi H, Al Balawi D, Khleifat KM, Aolymat I, Hamed S, et al. Enhanced efficacy of some antibiotics in the presence of silver nanoparticles against clinical isolate of Pseudomonas aeruginosa recovered from cystic fibrosis patients. Int J Nanomedicine. 2024;19:12461–12481. doi:10.2147/IJN.S479937
17. Haji SH, Ali FA, Aka STH. Synergistic antibacterial activity of silver nanoparticles biosynthesized by carbapenem-resistant Gram-negative bacilli. Sci Rep. 2022;12(1):15254. doi:10.1038/s41598-022-19698-0
18. Dove AS, Dzurny DI, Dees WR, Qin N, Nunez Rodriguez CC, Alt LA, et al. Silver nanoparticles enhance the efficacy of aminoglycosides against antibiotic-resistant bacteria. Front Microbiol. 2023;13:1064095. doi:10.3389/fmicb.2022.1064095
19. Pietsch F, Heidrich G, Nordholt N, Schreiber F. Prevalent synergy and antagonism among antibiotics and biocides in Pseudomonas aeruginosa. Front Microbiol. 2021;11:615618. doi:10.3389/fmicb.2020.615618
20. Ghytasi A, Hosseini Shekarabi SP, Rajabi Islami H, Shamsaie Mehrgan M. Dietary effects of lemon Citrus limon peel essential oil encapsulated in chitosan nanoparticles on hematological indices and antioxidant defense system of rainbow trout Oncorhynchus mykiss. Aquat Anim Nutr. 2021;7(1):27–41. doi: 10.22124/janb.2021.20348.1151.
21. Hanifi E, Ahmadifard N, Atashbar B, Meshkini S. Effects of zinc oxide nanoparticles on photosynthetic pigments, zinc accumulation, and activity of antioxidant enzymes of Dunalilla salina. Aquat Anim Nutr. 2022;8(4):31–42. doi: 10.22124/janb.2023.24071.1189.
22. Shamaei S, Ghaemi Sadr H. Biosynthesis of silver nanoparticles using Tagetes plant extracts: antimicrobial and anticancer activity assessment. Plant Biotechnol Persa. 2025;7(4):49–56. doi: 10.61186/pbp.7.3.175. Available from: http://pbp.medilam.ac.ir/article-1-250-en.html
23. Bagherzadeh Lakani F, Bazari Moghaddam S, Masoumzadeh M, Yousefi Jourdehi A, Jalilpoor J. Histopathology of dietary exposure to the selenium and iron nanoparticles on the liver tissue of reared beluga, Huso huso. Aquat Anim Nutr. 2023;9(1):11–25. doi: 10.22124/janb.2023.24281.1202.
24. Olajide OO, Emmanuel SA, Fayomi OM. Green synthesis, characterization, and in vivo anti-plasmodial activity of copper oxide nanoparticles using Moringa oleifera leaf extract. Journal of Biochemicals and Phytomedicine. 2025; 4(1): 31-39. doi: 10.34172/jbp.2025.5.
25. Bagherzadeh Lakani, F., Bazari Moghaddam,, S., Masoumzadeh, M., Yousefi Jourdehi, A., Jalilpoor, ,. Histopathology of dietary exposure of selenium and iron nanoparticles on the intestine in reared beluga (Huso huso). *Aquatic Animals Nutrition*, 2025; (): -. doi: 10.22124/janb.2025.29961.1283
26. Bagherzadeh Lakani F, Pajand Z, Mohseni M, Pourgholam MA, Pajand P. Effects of dietary selenium nanoparticles (Se-NPs) and iron nanoparticles (Fe-NPs) on growth performance and survival rate of Polychaeta, Hediste diversicolor. Aquat Anim Nutr. 2024;10(4):55–68. doi: 10.22124/janb.2025.29275.1266.

[DOI: 10.61882/pbp.8.1.12]